

DLTS measurements of radiation induced defects in epitaxial and MCz silicon detectors

F. Hönniger^{a,*}, E. Fretwurst^a, G. Lindström^a, G. Kramberger^b, I. Pintilie^c, R. Röder^d

^a*Institute for Experimental Physics, University of Hamburg, Germany*

^b*Josef Stefan Institute, University of Ljubljana, Slovenia*

^c*National Institute for Materials Physics, Bucharest, Romania*

^d*CiS Institut für Mikrosensorik gGmbH, Erfurt, Germany*

Available online 31 August 2007

Abstract

n-Type epitaxial silicon layers of different thickness and resistivity, grown on highly Sb doped CZ-substrate by ITME (Warsaw), and n-type MCz silicon supplied by Okmetic (Finland) were used for the processing of planar diodes at CiS (Erfurt). For the epi-diodes a standard as well as a diffusion oxygenation process was employed. Irradiations had been performed with 26 MeV protons at the cyclotron of the Karlsruhe University and with neutrons at the TRIGA reactor of the Ljubljana University. Microscopic investigations using the DLTS method were done. The correlation of the IO_{2i} -defect and the oxygen concentration was studied by a depth-profile measurement. The annealing behavior of the IO_{2i} -defect at different temperatures was investigated and the activation energy extracted. © 2007 Elsevier B.V. All rights reserved.

PACS: 85.30.De; 29.40.Wk; 29.40.Gx; 61.80.Jh; 61.82.Fk; 71.55.Cn

Keywords: Silicon detector; Radiation hardness; DLTS; Proton irradiation; Neutron irradiation; Defects; Oxygen dimer; IO_{2i}

1. Introduction

Silicon detectors will be largely employed in the tracking area of future colliding beam experiments. The proven technology and large-scale availability make them the favorite choice. However, the very large hadron fluence of up to 10^{16} hadrons per cm^2 expected for the upgrade of the Large Hadron Collider (S-LHC) will pose an unprecedented challenge as to their radiation tolerance [1]. Small-sized pixel detectors will be used in the innermost layers of the vertex detectors to cope with the much larger multiplicity of events. Thus a reduced thickness could be tolerated for keeping the capacitance at a low level. Thin detectors would then allow a much higher doping concentration at moderate depletion voltages. A large donor reservoir in n-type silicon would in turn delay the type inversion effect by radiation generated acceptors. These considerations had been the main motivation to start

systematic studies with diodes processed on thin epitaxial silicon layers [2–7]. On top of the expected benefits it was found that shallow bistable donors (BDs) are created by radiation in epi-diodes, compensating the build up of negative space charge by deep acceptors [6,7]. In Refs. [6,7] it is suggested that the radiation induced formation of BDs might be connected with the presence of oxygen dimers O_{2i} . The oxygen dimer is not electrically active and is, therefore, not detectable by Deep Level Transient Spectroscopy (DLTS). In principal it could be seen in IR absorption spectroscopy via its local vibration modes, however, only in thick homogeneous samples with a concentration exceeding 10^{15} cm^{-3} . The method is hence not applicable in thin epi-layers on Cz substrates [8]. As based on the assumption that the radiation induced IO_{2i} defect complex is formed via the reaction $\text{I} + \text{O}_{2i}$ the present work focuses on the relative estimation of the oxygen dimer concentration in different epitaxial and magnetic Czochralski (MCz) silicon via the detection of the IO_{2i} defect as measured by DLTS and its possible correlation with the oxygen content revealed by SIMS profiling.

*Corresponding author. Tel.: +49 4089984714.

E-mail address: frank.hoenniger@desy.de (F. Hönniger).

2. Experimental details

Silicon diodes manufactured on different kinds of epitaxial layers as well as on high resistivity MCz material were investigated in this work. The n-type epitaxial layers with thicknesses of 25 and 72 μm were grown on highly Sb doped Cz substrates by ITME [9] in Warsaw. The resistivity of the 25 μm layer was 50 Ωcm , while that of the 72 μm thick layer was 150 Ωcm . The 300 μm MCz wafers with a resistivity of nominal $>600 \Omega\text{cm}$ were produced by the company Okmetic [10] in Finland. The processing of the diodes had been performed by CiS [11]. For one batch of the 72 μm thick epi-layers a special heat treatment for 24 h at 1100 $^{\circ}\text{C}$ preceding the standard processing was implemented in order to increase the oxygen concentration in the epi-layer. Diodes produced this way are denoted as EPI-DO while the standard ones are indicated as EPI-ST. All diodes have the same p^+nn^+ structure with a p^+ electrode of 25 mm^2 surrounded by a 100 μm wide guard ring and an n^+ electrode with an area of 1 cm^2 given by the outer dimension of the device. Oxygen depth profiles have been measured by the SIMS-method [12] and are displayed in Fig. 1 for both epi-materials and for a 300 μm thick sample of a fully processed MCz wafer. The depth profiles of the EPI-DO and the MCz sample are quite similar with respect to the absolute values of the oxygen concentration as well as their shape, showing in both cases a homogenous distribution throughout the bulk material and a decrease of the oxygen concentration near to the surface, most likely caused by an out-diffusion of oxygen. On the other hand the oxygen concentration of the EPI-ST sample exhibits a strong non-homogeneous profile typically observed for samples of fully processed epi-layers without the DO option [5]. Irradiations had been performed with 26 MeV protons from the cyclotron of the University Karlsruhe and neutrons from the TRIGA reactor of the Jozef Stefan Institute in Ljubljana. All

fluences presented in this work are 1 MeV neutron equivalent values. The radiation induced defects have been studied using a Capacitance Deep Level Transient Fourier Spectroscopy (C-DLTFS) system manufactured by the company Phystech GmbH [13]. The standard DLTS spectra were recorded in a temperature range between 30 and 280 K.

3. Results and discussions

The DLTS spectra of a 72 μm EPI-ST and an EPI-DO diode, as irradiated with 26 MeV protons up to an equivalent fluence of $8.1 \times 10^{11} \text{cm}^{-2}$, are presented in Fig. 2. The DLTS peaks at about 200 and 120 K are typically observed in silicon after irradiation with charged hadrons or neutrons. They are attributed to both charge states of the divacancy ($V_2^{(-/0)}, V_2^{(=/-)}$), whereby the strong reduction of the $V_2^{(=/-)}$ signal compared with that of the single charge state $V_2^{(-/0)}$ is a well-known effect of hadron induced strain fields in heavily disordered regions [14–18]. This so-called cluster effect is the result of primary knocked on silicon atoms (PKAs) with high recoil energy generated by high energy hadrons. These PKAs lead to a defect cascade and at the end of the secondary displaced atoms disordered regions are created [19]. The slightly larger $V_2^{(-/0)}$ peak in the EPI-ST diode can most likely be attributed to a contribution of the E center (VP) which is created in the region of the EPI-ST sample where the oxygen profile exhibits a broad minimum (see Fig. 1). On the other hand the peak height of the vacancy–oxygen (VO) pair in EPI-ST material is a bit smaller compared to EPI-DO which is a further indication that the formation of single vacancy related defects (VP, VO) are influenced by the depth profile of the oxygen content in the EPI-ST material. But the most obvious difference between both spectra is the fact that the interstitial–dimer complex (IO_2) is only seen in the EPI-DO material while the carbon-interstitial

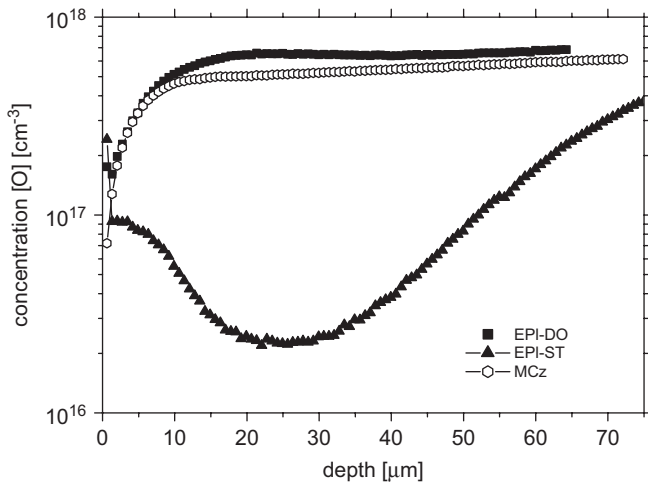


Fig. 1. Oxygen concentration profiles measured with SIMS for EPI-ST, EPI-DO and MCz diodes.

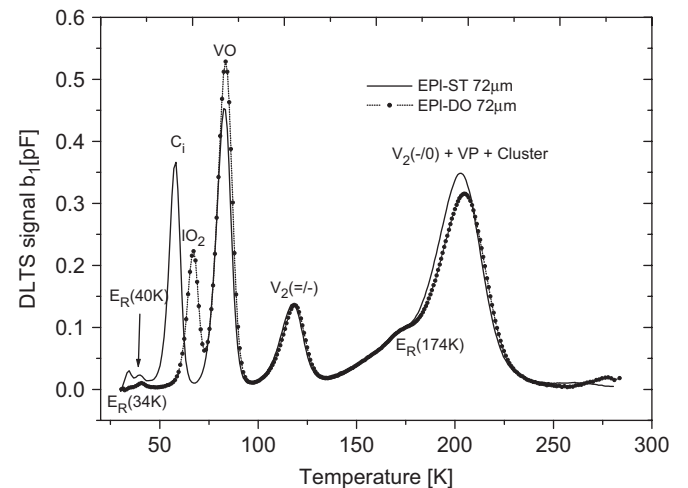


Fig. 2. DLTS spectra for EPI-ST and EPI-DO irradiated with 26 MeV protons with a fluence of $\Phi_{\text{eq}} = 8.1 \times 10^{11} \text{cm}^{-2}$. $U_R = -20 \text{V}$, $U_P = -0.1 \text{V}$, $t_p = 100 \text{ms}$, $T_W = 200 \text{ms}$.

defect (C_i) is only detected in the EPI-ST sample. The formation of the IO_{2i} defect evidences the presence of O_{2i} in the epi-material with a high oxygen concentration. The fact that C_i is not seen in EPI-DO does not indicate that the carbon content of this material is much smaller than in the EPI-ST material; it is only an effect of the higher probability for the formation of C_iO_i in the EPI-DO material due to its higher oxygen concentration compared to the standard material [15]. It should be mentioned here that the carbon content in this epi-material has been measured by SIMS and was found to be about $3 \times 10^{15} \text{ cm}^{-3}$, which is the detection limit of the method. Hence we can only state that the carbon concentration is not larger than $3 \times 10^{15} \text{ cm}^{-3}$ and may be very well even much below that value. But there are no arguments for a variation in the carbon concentration in both epi-materials EPI-ST and EPI-DO, respectively. Also a possible introduction of carbon during the diode processing can be excluded. On the other hand from the absence of the IO_{2i} signal in the EPI-ST diode it cannot be concluded that oxygen dimers are not present in this material. The IO_{2i} is not visible due to the filling conditions for the traps ($U_R = -20 \text{ V}$, $U_p = -0.1 \text{ V}$) chosen for recording the spectra shown in Fig. 2. This way only defects in a depth between about 5 and $33 \mu\text{m}$ from the p^+ contact are detected. In this region the O_{2i} concentration in the EPI-ST material is expected to be very small since the oxygen concentration is low. But near to the interface between the epi-layer and the Cz substrate the oxygen concentration is much higher (see Fig. 1). Therefore, it is expected that the O_{2i} concentration in this region is also higher compared to the front region and the IO_{2i} should become visible. In fact, this is demonstrated in Fig. 3 where the spectrum of the EPI-ST diode, shown in Fig. 2 (front region), is compared with a spectrum recorded under filling conditions which

corresponds to a depletion region near to the interface. It is also obvious that in this region with its high oxygen concentration the C_i defect is not visible anymore pointing to the argument given above for the absence of a C_i signal in EPI-DO. In order to get more insight into the formation of the IO_{2i} and its dependence on the oxygen concentration, depth profiles were measured not only for the EPI-ST material but also for the EPI-DO and the MCz material which exhibit an almost homogenous oxygen distribution throughout the bulk. Before presenting the measured IO_{2i} depth profiles it is noted that the DLTS spectrum of a MCz diode after irradiation with 26 MeV protons is very similar to that recorded for the EPI-DO sample (see Fig. 4). Especially a clear IO_{2i} signal is seen and no C_i signal. In Fig. 4 a spectrum before irradiation is included, which shows two small peaks located at about 112 and 62 K. While the 112 K peak cannot be attributed to a known defect, the signal at 62 K is most likely related to a thermal doubledonor TDD. This assignment is based on a direct capture cross-section measurement resulting in a very large value of $\sigma_n = 1 \times 10^{-12} \text{ cm}^2$ which is expected for a shallow double donor. The IO_{2i} depth profiles were extracted from transient measurements, recorded at a constant temperature of 67 K, varying the reverse bias and the pulse bias accordingly and using a time window T_W of 200 ms. In Fig. 5 the depth profiles of the IO_{2i} concentration are plotted for all three materials. As expected, the profiles of the MCz and the EPI-DO material are nearly flat in the measured region with the exception of the first point of the MCz material near to the p^+ surface. But the profile of the EPI-ST material reflects the non-homogeneity of the oxygen profile as measured by SIMS. This correlation between the respective IO_{2i} and O_i concentration has led to the question whether the measured IO_{2i} concentration can be taken as a relative measure of the oxygen-dimer

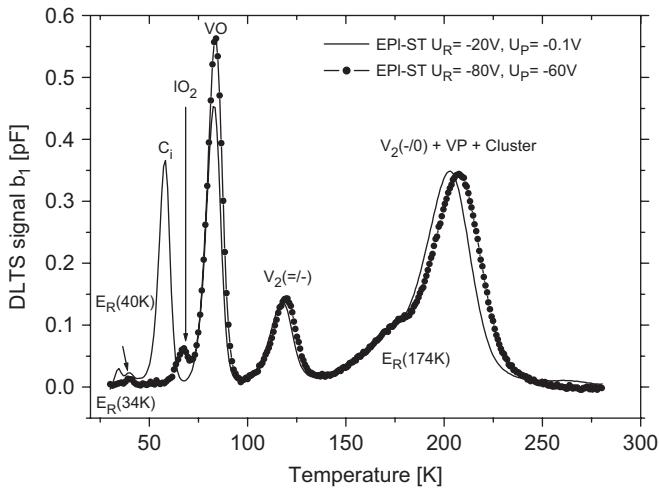


Fig. 3. DLTS spectra for EPI-ST irradiated with 26 MeV protons with a fluence of $\Phi_{eq} = 8.1 \times 10^{11} \text{ cm}^{-2}$. Comparison of DLTS measurements close to the substrate ($U_R = -80 \text{ V}$, $U_p = -60 \text{ V}$) and in the region of low oxygen concentration ($U_R = -20 \text{ V}$, $U_p = -0.1 \text{ V}$), $t_p = 100 \text{ ms}$, $T_W = 200 \text{ ms}$.

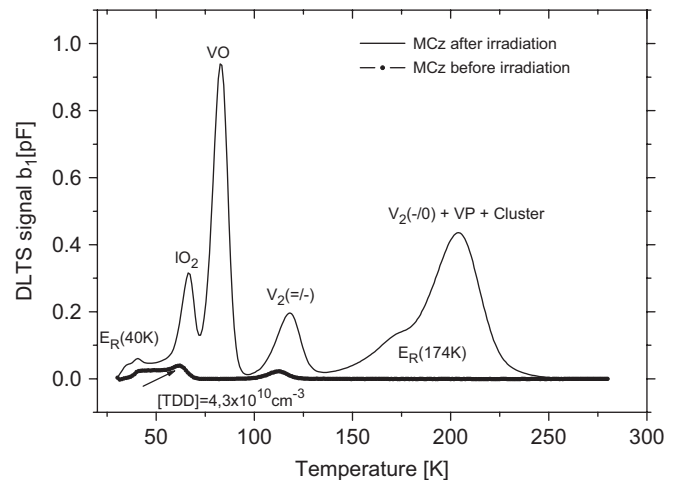


Fig. 4. DLTS spectra for MCz material before and after irradiation with 26 MeV protons with a fluence $\Phi_{eq} = 4.6 \times 10^{11} \text{ cm}^{-2}$. $U_R = -20 \text{ V}$, $U_p = -5 \text{ V}$, $t_p = 100 \text{ ms}$, $T_W = 200 \text{ ms}$.

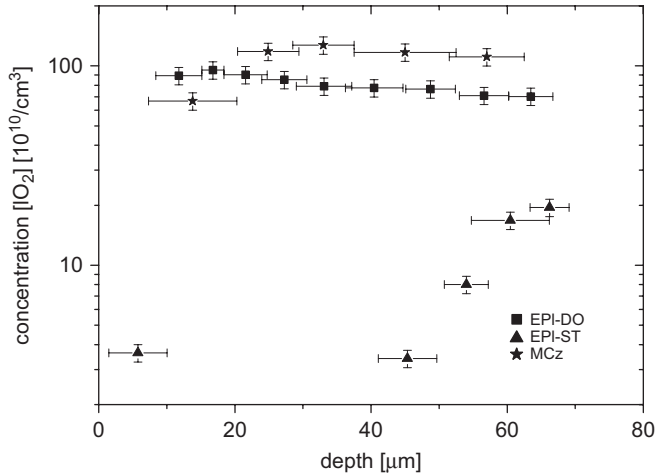


Fig. 5. Depth profiles of IO_{2i} defect concentration in EPI-ST, EPI-DO and MCz after irradiation with 26 MeV protons with fluences of $\Phi_{\text{eq}} = 8.1 \times 10^{11} \text{ cm}^{-2}$, $\Phi_{\text{eq}} = 4.8 \times 10^{11} \text{ cm}^{-2}$ and $\Phi_{\text{eq}} = 4.6 \times 10^{11} \text{ cm}^{-2}$ accordingly. All concentrations are scaled to $\Phi_{\text{eq}} = 8.1 \times 10^{11} \text{ cm}^{-2}$.

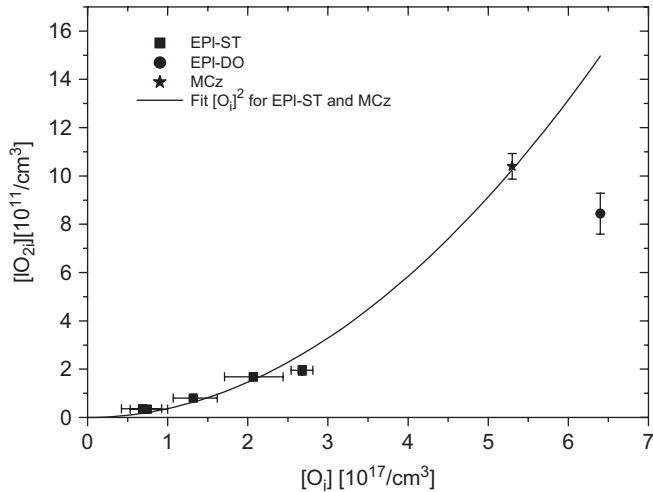


Fig. 6. Concentration of the IO_{2i} defect in EPI-ST, EPI-DO and MCz detectors as function of the oxygen concentration. The solid line represents a fit with a quadratic function.

concentration itself in this material. If we assume that the formation of IO_{2i} is not disturbed by the competing reaction $\text{I} + \text{C}_s \rightarrow \text{Si}_s + \text{C}_i$ or other interstitial related defect reactions like the formation of I_2O_{2i} [20] the IO_{2i} concentration should reflect the oxygen-dimer content in the material ($\text{I} + \text{O}_{2i} \rightarrow \text{IO}_{2i}$). IR absorption measurements by Murin et al. [8] showed a quadratic dependence of the oxygen dimer concentration on the O_i content in oxygen-rich Cz silicon. In Fig. 6 the correlation between the IO_{2i} and the oxygen concentration for all measured samples (EPI-ST, EPI-DO, MCz) is plotted. In case of the Epi-ST and the MCz sample a quadratic dependence as suggested by the Murin result [8] can be shown. However, this quadratic function does not reproduce the value observed for EPI-DO, which is only about 50% of the expected concentration. This finding is so far not understood.

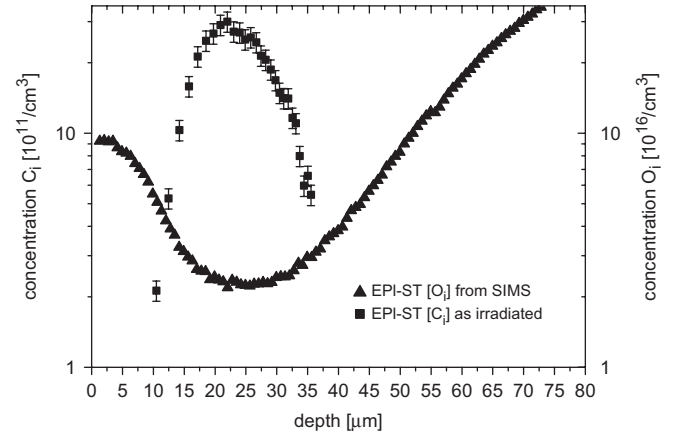


Fig. 7. Depth profile of the C_i concentration in a EPI-ST detector irradiated with 26 MeV protons with a fluence of $\Phi_{\text{eq}} = 8.1 \times 10^{11} \text{ cm}^{-2}$ and correlated with the oxygen concentration.

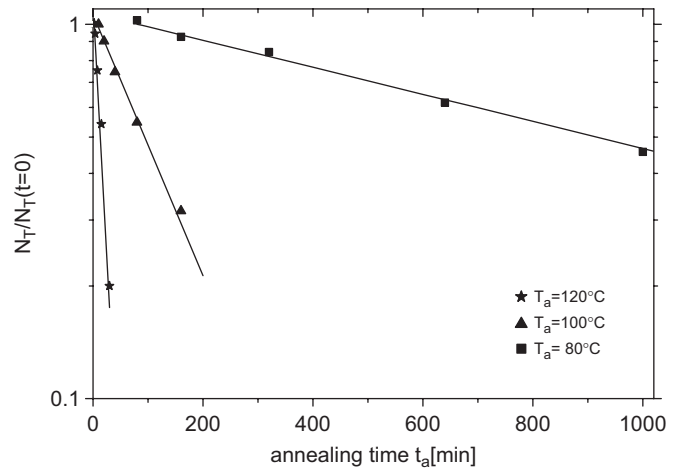


Fig. 8. Isothermal annealing of the IO_{2i} defect at different temperatures T_a . Measurement performed on a $25 \mu\text{m}$ EPI-ST detector irradiated with $\Phi_{\text{eq}} = 1 \times 10^{12} \text{ cm}^{-2}$ reactor neutrons. $U_R = -20 \text{ V}$, $U_P = -0.1 \text{ V}$, $t_P = 100 \text{ ms}$, $T_W = 200 \text{ ms}$.

In addition to the non-homogeneous IO_{2i} depth profile we found also a strong variation in the C_i concentration as function of the depleted depth in the EPI-ST material, as demonstrated in Fig. 7. The $[\text{C}_i]$ profile has a maximum at a depth where the oxygen concentration has its minimum. Toward the regions with a higher oxygen concentration the $[\text{C}_i]$ drops down rapidly. This rapid decrease is due to the high capture rate of C_i by O_i forming the C_iO_i complex, when the O_i concentration is sufficiently large. The competing reaction $\text{C}_i + \text{C}_s \rightarrow \text{C}_i\text{C}_s$ plays a minor role, since the concentration of C_s is much smaller than the oxygen concentration as mentioned before. It should also be reminded that the C_i is mobile at room temperature (RT) and cannot be detected anymore, if the sample is stored for a prolonged period at RT (the annealing time constant at RT is about four days for carbon and oxygen lean material [14]).

Isothermal annealing studies of the IO_{2i} defect complex at different temperatures have been performed for the first time in this work. For this annealing experiment EPI-ST

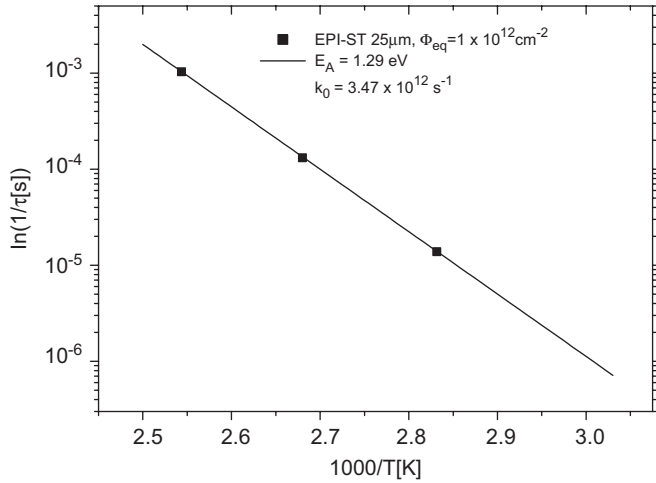


Fig. 9. Arrhenius plot for the thermal activation of the IO_{2i} defect after irradiation with $\Phi_{\text{eq}} = 1 \times 10^{12} \text{ cm}^{-2}$ reactor neutrons. EPI-ST samples with 25 μm thick layer.

diodes with a thickness of 25 μm were irradiated with neutrons up to $1 \times 10^{12} \text{ cm}^{-2}$ and annealed at 80, 100 and 120 °C. The annealing data for the three mentioned temperatures are displayed in Fig. 8 together with their fits. The Arrhenius plot of the extracted time constants shown in Fig. 9 revealed

$$1/\tau = k(T) = k_0 \cdot e^{-E_A/k_B \cdot T} \quad (1)$$

with a frequency factor $k_0 = 3 \times 10^{12} \text{ s}^{-1}$ and an activation energy $E_A = 1.29 \text{ eV}$. Thus, with a first-order kinetics and a frequency factor k_0 close to the most abundant phonon frequency, it is very likely that the annealing of the IO_{2i} defect is due to dissociation.

4. Conclusions

Detailed DLTS studies on proton and neutron irradiated epitaxial silicon layers with and without a deliberate oxygen enrichment have been performed. For comparison also oxygen-rich MCz silicon was included in these investigations. The concentration of the radiation induced interstitial-oxygen dimer defect complex IO_{2i} had been studied in correlation with the respective oxygen content. The results for the epi-sample without oxygen enrichment and the MCz sample suggested a quadratic dependence as expected from the IR results on oxygen dimers. However, for the oxygen enriched epi-sample only 50% of the expected value had been measured, a result which is not yet understood. In addition the activation energy for the annealing of the IO_{2i} defect was determined for the first time from isothermal annealing experiments at different temperatures resulting in a value of $E_A = 1.29 \text{ eV}$, and the extracted frequency factor $k_0 = 3 \times 10^{12} \text{ s}^{-1}$, indicating that the annealing is most likely a dissociation process. Finally, also the C_i concentration in the standard epi-sample was measured to be strongly anticorrelated with the oxygen concentration, a result easily understood as due to the formation of $C_i\text{O}_i$.

Acknowledgments

One of the authors (Ioana Pintilie) expresses many thanks to the Alexander von Humboldt foundation for obtaining a research fellowship, which enabled her participation in this project. This work was performed in the frame of the CiS-MUZ project under contract 0518/03/05 and within the CERN-RD50 collaboration. Many thanks are due to the team of the research reactor of the Jozef Stefan Institute in Ljubljana for the neutron irradiation and to A. Furgeri and the team at the cyclotron of the University of Karlsruhe for the proton irradiation. We are especially grateful to E. Nossarzewska at ITME for providing the epi-material and performing spreading resistance measurements. A. Barcz from the Physics Institute of the Polish Academy of Sciences in Warsaw had executed the very reliable SIMS measurements and we like to express many thanks for his work and numerous discussions.

References

- [1] F. Giannotti, M.L. Mangano, T. Virdee, et al., Physics potential and experimental challenges of the LHC luminosity upgrade, hep-ph/0204087, CERN-TH/2002-078, April 2002.
- [2] G. Kramberger, D. Contarato, E. Fretwurst, F. Hönniger, G. Lindström, I. Pintilie, R. Röder, A. Schramm, J. Stahl, Nucl. Instr. and Meth. A 515 (2003) 665.
- [3] G. Lindström, E. Fretwurst, F. Hönniger, G. Kramberger, M. Möller-Ivens, I. Pintilie, A. Schramm, Nucl. Instr. and Meth. A 556 (2006) 451.
- [4] G. Kramberger, V. Cindro, I. Dolenc, E. Fretwurst, G. Lindström, I. Mandic, M. Mikuz, M. Zavrtanik, Nucl. Instr. and Meth. A 554 (2005) 212.
- [5] G. Lindström, I. Dolenc, E. Fretwurst, F. Hönniger, G. Kramberger, et al., Nucl. Instr. and Meth. A 568 (2006) 66.
- [6] I. Pintilie, E. Fretwurst, F. Hönniger, G. Lindström, J. Stahl, Nucl. Instr. and Meth. A 552 (2005) 56.
- [7] I. Pintilie, M. Buda, E. Fretwurst, G. Lindström, J. Stahl, Nucl. Instr. and Meth. A 556 (2006) 197.
- [8] L.I. Murin, T. Hallberg, V.P. Markevich, J.L. Lindström, Phys. Rev. Lett. 80 (1) (1998) 93.
- [9] ITME, Institute for Electronics Materials Technology, Warsaw, Poland.
- [10] Okmetic Oyj, Vantaa, Finland.
- [11] CiS Institut für Mikrosensorik gGmbH, Erfurt, Germany.
- [12] A. Barcz SIMS laboratory, Institute of Physics, Warsaw, Poland.
- [13] Phystech GmbH, (www.phystech.de), Moosburg, Germany.
- [14] M. Moll, Radiation damage in silicon particle detectors, Ph.D. Thesis, University of Hamburg, 1999.
- [15] M. Kuhnke, Microscopic investigations on various silicon materials irradiated with different particles with the DLTS method, Ph.D. Thesis, University of Hamburg, 2001.
- [16] B.G. Svensson, B. Mohadjeri, A. Hallén, J.V. Svensson, J.W. Corbett, Phys. Rev. B 43 (1991) 2292.
- [17] B.G. Svensson, C. Jagadish, A. Hallén, J. Lalita, Phys. Rev. B 55 (1997) 10498.
- [18] M. Moll, E. Fretwurst, M. Kuhnke, G. Lindström, Nucl. Instr. and Meth. B 186 (2002) 100.
- [19] G.P. Mueller, N.D. Wilsey, M. Rosen, IEEE Trans. Nucl. Sci. NS-29 (6) (1982) 1493.
- [20] J.L. Lindström, T. Hallberg, J.G. Hermansson, L.I. Murin, B.A. Komarov, V.P. Markevich, M. Kleverman, B.G. Svensson, Physica B 308–310 (2001) 284.